JACS
JOURNAL OF THE AMERICAN CHEMICAL SOCIETY
Article
pubs.acs.org/JACS

The Real Role of N-Heterocyclic Carbene in Reductive Functionalization of CO_2: An Alternative Understanding from Density Functional Theory Study

Qinghai Zhou and Yuxue Li*

State Key Laboratory of Organometallic Chemistry, Shanghai Institute of Organic Chemistry, Chinese Academy of Sciences, 345 Lingling Road, Shanghai 200032, P. R. China

Supporting Information

ABSTRACT: The mechanisms of reductive functionalization of CO_2 to formamide catalyzed by N-heterocyclic carbene (NHC) were comprehensively studied with DFT calculations. New activation mode with much lower energy barrier than those proposed before was discovered. In this reaction, NHC acts as neither a CO_2 nor a silane activator, but as a precursor of the real catalyst, i.e., the *in situ* formed ionic liquid $[NHCH]^+[Carbamate]^-$. In this loose contact ion pair, the negatively charged O atom of the carbamate anion becomes the new active site and is free to do nucleophilic attack. When amine is absent, CO_2 will be converted into methanol. In this case, the NHC-CO_2 adduct is the real catalytic species, the active site shifted from the carbene C atom to the negatively charged O atom. These new activation modes follow a pattern of "S_N2@Si-Acceptor", in which the Si−H bond is activated via concerted backside S_N2 nucleophilic attack by the negatively charged O atom, and the leaving hydride is directly accepted by a free CO_2 molecule. The advantages of these new activation modes originate from the following points: (1) The ionic liquid $[NHCH]^+[Carbamate]^-$ and NHC-CO_2 adduct are thermodynamically more stable than NHC. (2) The active site of the NHC catalyst is extended outside a lot. Consequently, the large steric effect between the NHC arms and the substrates in transition state can be avoided to some extent. (3) The O atom has good silicon affinity. In addition, a free CO_2 molecule, whose carbon atom is more electrophilic than those of the CO_2 moieties in NHC-CO_2 adduct and carbamate, acts as an efficient hydride acceptor.

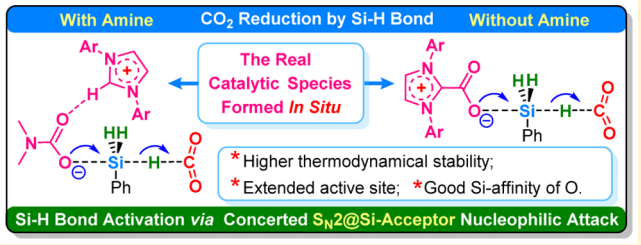

1. INTRODUCTION

Nowadays, CO_2 is a hot research focus both as a greenhouse gas causing global warming problems and an attractive, nontoxic, abundant C1 building block.[1] In the development of CO_2 transformation and utilization reactions, N-heterocyclic carbenes (NHCs)[2−5] and guanidines[6] are promising metal-free organocatalysts.

In 2012, Cantat et al. reported the NHC-catalyzed reductive functionalization of CO_2 into formamides with silanes as reductant and amines as functionalizing reagents.[3a] The reaction proceeds well at room temperature and 1.0 bar CO_2 (Scheme 1, reaction **1**). A little earlier, this reaction was achieved with 1,5,7-triazabicyclo[4.4.0]dec-5-ene (TBD) catalyst under harsher conditions (100 °C and 2 bar).[6g] And as early as 2009, Ying et al. reported the conversion of CO_2 into methanol with silanes and NHC catalyst under room temperature and ambient pressure (Scheme 1, reaction **2**).[3b] Very recently, methylamines and methane have been achieved from reductive functionalization of CO_2.[4] These reductive approaches are of great importance for enlarging the spectrum of compounds directly from CO_2. Therefore, a deep understanding of the mechanism is very important both for improving CO_2 transformation reactions and for NHC catalyst design.

Scheme 1. Reaction 1: Reductive Functionalization of CO_2 into Formamide Catalyzed by IPr and Reaction 2: Reduction of CO_2 into Methanol Catalyzed by IMes-CO_2

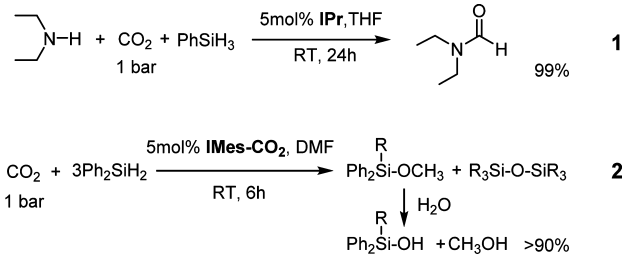

As shown in Scheme 2, several mechanisms for the CO_2 reduction process have been already proposed and studied since 2009.[3,5] Two types of activation modes, i.e., silane-activation (mode **A**[3b,5a,b]) and CO_2-activation modes (modes **B**,[3b,5a,b] **C**,[5c] and **D**[5b,6g]) with NHC as the catalyst species have been reported. However, based on comprehensive DFT studies, we found new activation modes **E** and **F** that are much more

Received: April 8, 2015
Published: July 29, 2015

DOI: 10.1021/jacs.5b03651
J. Am. Chem. Soc. 2015, 137, 10182−10189

Scheme 2. (a) Previously Proposed Activation Modes for NHC Catalyzed Reduction of CO_2 by Silane and (b) New Activation Modes Proposed in This Work

(a) Previously Proposed Activation Modes:

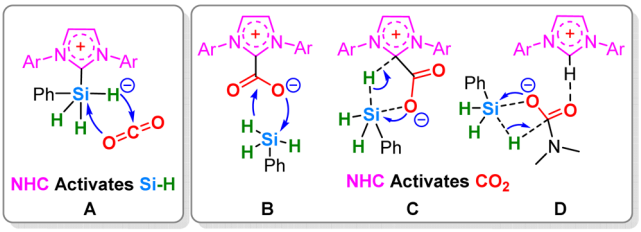

(b) New Activation Modes Proposed In This Work:

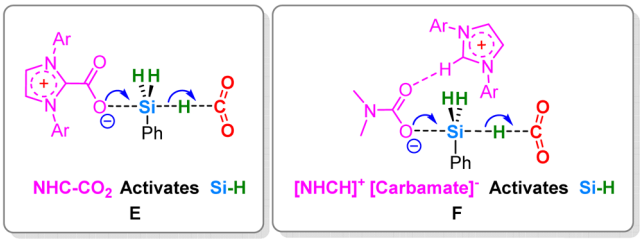

favorable than modes **A**–**D**. In activation modes **E** and **F**, the thermodynamically more stable NHC-CO_2 adduct and the ionic liquid $[NHCH]^+[Carbamate]^-$, rather than NHC, are the real catalytic species, respectively. In this new mechanism, two instead of one CO_2 react. The first becomes a NHC-CO_2 adduct or carbamate, while the second binds as the CO_2 to be reduced.

In terms of reaction mechanisms, reaction **2** is a simplified case of reaction **1** because no amine is involved. Therefore, in the main text, first we concentrate on reaction **1**, and then reaction **2** is discussed concisely. Our results present new insights into the catalytic mechanisms and will challenge the generally accepted understandings.

2. MODELS AND METHODS

To disclose the reaction mechanisms, DFT[7] studies using the M06[8] method with Gaussian09[9] program have been performed. The M06 method was proved to be efficient and reliable in mechanistic studies of organic system with nonbonding interactions. In the calculation models, the 6-31G* basis set was used for the 2,6-diisopropylphenyl and 2,4,6-trimethylphenyl substituent groups of IPr and IMes, respectively; and the large 6-311++G** basis set was used for the rest part (the core part). Ultrafine integral grid was used to get more accurate results. Me_2NH was used as the calculation model for the amine substrates. All geometries were fully optimized in solvent with SMD[10] method (THF for reaction **1**, ε = 7.4257; DMF for reaction **2**, ε = 37.219). Harmonic vibrational frequency calculations show that the stationary points located were either minima (with zero imaginary frequencies) or transition states (with one imaginary frequency). Important transition states have been checked by intrinsic reaction coordinate (IRC) calculations.[11] The 3D molecular figures were prepared using CYLView.[12]

For a reaction where the number of molecules of the reactant and the product are not equal, the translational and rotational entropy loss in the transition state will be overestimated significantly if the separated reactants were used as the energy reference, and the calculated barrier will be too high. However, if the reactant complex is used as the energy reference, the entropy loss caused by the binding will be underestimated, and the calculated barrier will be too low. In this study, the separated reactants were used as the zero reference. Meanwhile, corrections were made to the calculated free energies based on "the theory of free volume",[13] i.e., for 2-to-1 (or 1-to-2) reactions, a correction of −2.6 (or 2.6) kcal/mol was made.

3. RESULTS AND DISCUSSION

3.1. The Mechanism of Reaction 1. *3.1.1. The Pre-Equilibrium of CO_2-Amine System.* In neat liquid or dry solvents, amine can react easily with CO_2 leading to carbamic acids or ammonium carbamate salts.[14] For example, in an ice-cooled bath, dimethylamine reacts with dry CO_2 in anhydrous dichloromethane yielding the product dimethylammonium dimethylcarbamate,[14a] which has been isolated and characterized by X-ray diffraction.[15a] For the reaction of Me_2NH and CO_2 in a 2:1 ratio, a barrier of 9.5 kcal/mol has been reported,[16a] which is also qualitatively consistent with our results (12.8 kcal/mol).[17] These results indicate that there is a fast pre-equilibrium of CO_2 and Me_2NH in advance of the CO_2 reduction. Therefore, the pre-equilibrium under the presence of IPr was first explored and is shown in Scheme 3.

IPr-R is the zero energy reference containing separated IPr, Me_2NH, and CO_2 molecules. Along *Path-a*, under the activation of IPr, the nucleophilic attack of Me_2NH to CO_2

Scheme 3. Calculated Reaction Pathways of the Pre-Equilibrium of CO_2-Amine-IPr System[a]

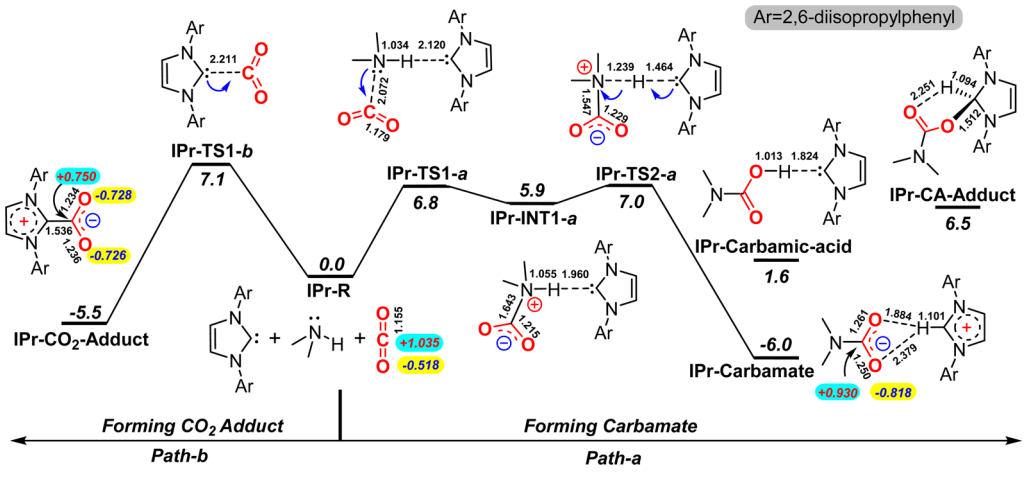

[a]The relative free energies (ΔG_{sol}, 298 K, 1.0 atm) in THF are in kcal/mol. The selected bond lengths are in Å, the selected NPA atomic charges are given in red (positive) and blue (negative) numbers. Calculated at the M06/(6-311++G** and 6-31G*) level.

DOI: 10.1021/jacs.5b03651
J. Am. Chem. Soc. 2015, 137, 10182−10189

Scheme 4. Calculated Reduction Transition States of Different Activation Modes for Reaction 1 (Catalyzed by IPr, Ar = 2,6-diisopropylphenyl)[a]

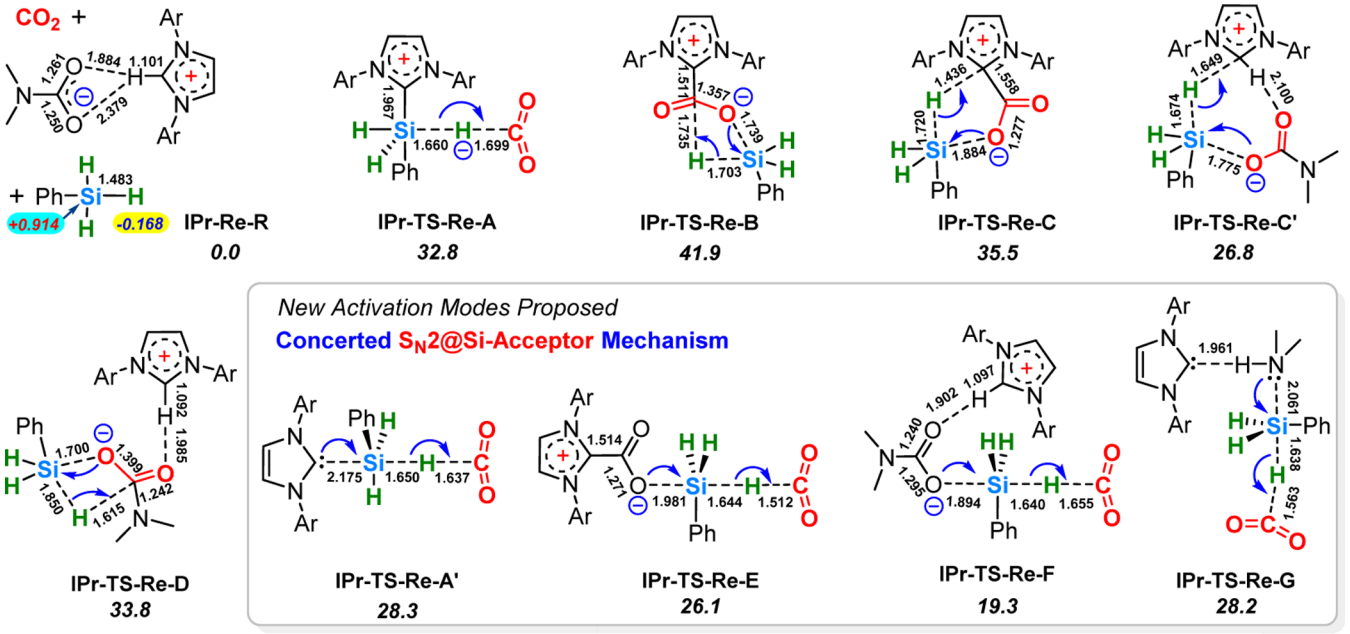

[a]The relative free energies (ΔG_{sol}, 298 K, 1.0 atm) in THF are in kcal/mol. The selected bond lengths are in Å, the selected NPA charges are given in red (positive) and blue (negative) numbers. Calculated at the M06/(6-311++G** and 6-31G*) level.

(**IPr-TS1-*a***, 6.8 kcal/mol) leads to the zwitterionic carbamate species **IPr-INT1-*a*** (5.9 kcal/mol), in which the Me_2NH^+-CO_2^- adduct forms hydrogen bond with IPr. The subsequent proton transfer (**IPr-TS2-*a***, 7.0 kcal/mol) generates the stable IPr-carbamate salt complex (**IPr-Carbamate**, −6.0 kcal/mol), a contact ion pair ($[IPrH]^+[Carbamate]^-$), which is more stable than the neutral IPr-carbamic acid complex (**IPr-Carbamic-acid**, 1.6 kcal/mol) due to the large proton affinity of IPr. The adduct of carbamic acid to IPr (**IPr-CA-Adduct**, 6.5 kcal/mol) is much less favorable. **IPr-Carbamate** and alkylammonium alkylcarbamates are actually ionic liquids (ILs).[18] In **IPr-Carbamate** the imidazolium and the carbamate anion are combined via hydrogen bond. Along with *Path-b*, CO_2 is captured by IPr over transition state **IPr-TS1-*b*** (7.1 kcal/mol), forming **IPr-CO_2-Adduct** (−5.5 kcal/mol). The overall barrier of *Path-a* is much lower than that of the uncatalyzed reaction (12.8 kcal/mol),[17] indicating that IPr accelerates the carbamate formation. In experiments, **IMes-CO_2** and **IPr-CO_2** adducts can be synthesized under room temperature and ambient pressure and have been characterized by X-ray diffraction.[2k,19c] The low transformation barriers (<13.0 kcal/mol) indicate that it is a fast equilibrium, and the IPr catalyst will be trapped in advance of the CO_2 reduction. Therefore, the **IPr-Carbamate** complex or **IMes-CO_2-Adduct** should be considered as the zero energy reference for the following reduction processes of reactions **1** and **2**, respectively.

3.1.2. The Activation Modes in Reaction 1. In the previous DFT calculations, some studies[5a,b] show that **A** is the most favorable activation mode. In another study,[5c] however, mode **C** was proposed to be the best. Furthermore, these calculations have been performed using different methods and basis sets. Therefore, to do a reliable comparison, it is necessary to recalculate all these activation modes at the same level of theory.

In the reaction, small molecules may be generated during the regeneration of the IPr catalyst, such as carbamate acid or CO_2. However, they may not participate in the following reaction step and hence do not need to be bound. Transition states without such small molecules (the "partial model") are given in Scheme 4, and their relative energies were calculated by model reactions of releasing the small molecules. Transition states with these small molecules, i.e., the "whole model", for which all the transition states have the same composition, are given in Scheme S2.[17]

As shown in Scheme 4, the stable $[IPrH]^+[Carbamate]^-$ salt complex **IPr-Carbamate**, the free $PhSiH_3$, and CO_2 molecules were used as the zero energy reference (**IPr-Re-R**). In activation mode **A** (**IPr-TS-Re-A**, 32.8 kcal/mol), NHC activates the Si−H bond by forming C−Si bond, pushing more electron density to the H atom and thus promoting the hydride transfer to the electrophilic carbon center of CO_2.[5a,b] This mechanism can be considered as the classical S_N2@Si pathway, for which a deep understanding has been presented by Bickelhaupt et al.[20,21] The NHC and the silane first form a penta-coordinated Si intermediate, then the Si−H bond breaks and the hydride attacks the CO_2. In mode **B** (**IPr-TS-Re-B**, 41.9 kcal/mol), the CO_2 moiety of the IPr-CO_2 adduct is directly reduced. In the IPr-CO_2 adduct, the O atom of the CO_2 moiety has increased negative NPA[22] atomic charges (−0.728 vs −0.518 in free CO_2, Scheme 3) and becomes more ready to attack the positive Si center. However, the carbon atom of the CO_2 moiety has decreased positive charges (+0.750 vs +1.035 in free CO_2, Scheme 3) and becomes reluctant to accept a hydride. In activation mode **C** (**IPr-TS-Re-C**, 35.5 kcal/mol), the hydride transfers to the NHC carbene carbon atom via a five-membered ring transition state under the attack of the CO_2 moiety, and the subsequent 1,2-H shift yields the formoxysilane.[5c,17] In activation mode **D** (**IPr-TS-Re-D**, 33.8

DOI: 10.1021/jacs.5b03651
J. Am. Chem. Soc. 2015, 137, 10182−10189

kcal/mol), the CO_2 moiety in carbamate salt intermediate is directly reduced by silane.[5b,6g]

The above calculation results show that the barriers of these previously proposed activation modes **A** to **D** are much higher than the expected value of around 20 kcal/mol considering the mild experimental conditions. Therefore, more reasonable activation modes need to be found out.

Activation modes **A** to **D** indicate that a nucleophilic attack at the Si center will promote the Si−H bond cleavage,[20] increasing the reactivity of the hydride. It is well-known that oxygen has good silicon affinity. Therefore, the species with negatively charged O atom, such as the IPr-CO_2 adduct and the $[IPrH]^+[Carbamate]^-$ intermediate, are expected to be able to activate the Si−H bond effectively. The O−Si bond (122.6 kcal/mol) is much stronger than N−Si and C−Si bond (97.5 and 94.4 kcal/mol, respectively).[23] The favorable formation of O−Si bond drives many organic reactions, such as the Brook rearrangement and Peterson olefination.[24] It is also well-known that fluoride is a powerful reagent to remove silicon groups with the driving force to form the strong F−Si bond (159.9 kcal/mol).[21,23]

We found that the high barriers of activation modes **B**, **C**, and **D** come from the following aspects: (1) The most favorable nucleophilic attack is a backside S_N2 attack, rather than a side attack; and the strain in the four-/five-membered ring transition states may also increase the barrier. This point of view is supported by **IPr-TS-Re-A′** (28.3 kcal/mol), a linear S_N2 attack version of **IPr-TS-Re-A**, which has a barrier decrease by 4.5 kcal/mol. (2) The carbon atoms of CO_2 moieties in IPr-CO_2 adduct and carbamate intermediate are actually deactivated to some extent, as indicated by the atomic charges (+0.750, + 0.930, vs +1.035 in free CO_2, Scheme 3). The carbon atom in a free CO_2 is more electrophilic and more ready to accept a hydride. In addition, the N atom of the amine substrate can also do nucleophilic attack at the Si center, thus more activation modes need to be checked.

These notions inspired us to design a new activation mode and find out the true function of the NHC catalyst in this reaction. If the amine substrate is not involved, an optimal activation mode **E** (**IPr-TS-Re-E**, 26.1 kcal/mol) was proposed, in which the negatively charged O atom of the IPr-CO_2 adduct activates the Si−H bond via backside S_N2 attack, and the leaving hydride directly attacks a free CO_2 molecule. As far as we know, this model has never been proposed and tested. The calculated barrier drops by 6.7 kcal/mol relative to activation mode **A** (**IPr-TS-Re-A**). Subsequently, following the same rule, activation mode **F** (**IPr-TS-Re-F**, 19.3 kcal/mol) was proposed, in which the negatively charged O atom of the carbamate anion in $[IPrH]^+[Carbamate]^-$ ion pair activates the Si−H bond via a concerted linear backside S_N2 attack, and the free CO_2 acts as a hydride acceptor. The barrier drops as much as 13.5 kcal/mol compared with **IPr-TS-Re-A**. This concerted "S_N2@Si-Acceptor" Si−H bond activation mode is also supported by other experiments, such as the $B(C_6F_5)_3$-catalyzed hydrosilylation of carbonyl compounds[20b] and the silylation of the carbamate with trimethylchlorosilane.[14a] And this type of transition state also has been reported by Wang et al. in a recent theoretical study.[20d]

Scheme 5 shows a comparison of the classical and the "S_N2@Si-Acceptor" activation modes of hydrosilanes. As shown in Scheme 5a, the classical activation mechanism of hydrosilanes is stepwised, with the penta-coordinated Si intermediate formation: the Nu-Si bond forms first, leading to the penta-coordinated Si intermediate (**INT**), then the Si−H bond breaks, and the hydride attacks the CO_2. However, the "S_N2@Si-Acceptor" mechanism is a concerted, one-step process, without intermediate formation. The Nu−Si bond formation, the Si−H bond break, and the H−C bond formation take place at the same time. When the nucleophilic attack occurs, it is the existence of the hydride acceptor that changes the PES from (**a**) to (**b**). In addition, the "S_N2@Si-Acceptor" mechanism in our study is more favorable than the classical activation mechanism. For example, **IPr-TS-Re-A′** is 4.5 kcal/mol lower than **IPr-TS-Re-A**. And the IRC calculations of **IPr-TS-Re-A′** and **IPr-TS-Re-A** show the difference between these two mechanisms clearly.[17]

Scheme 5. Classical (a) and the "S_N2@Si-Acceptor" (b) Activation of Hydrosilanes

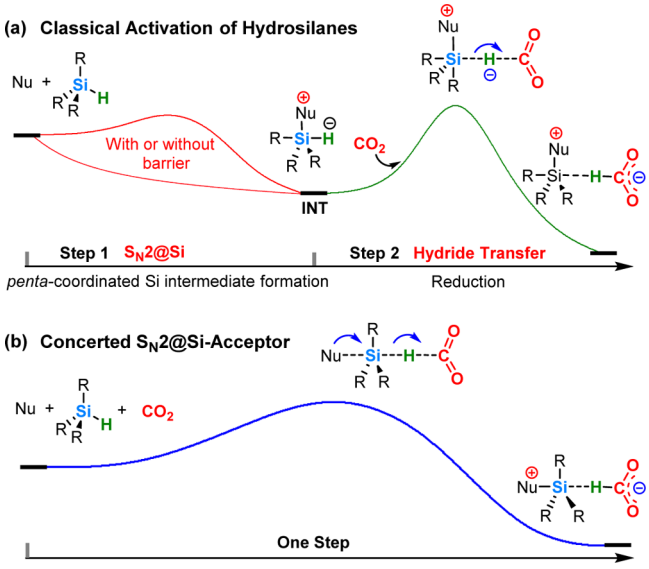

Now we rethink the origin of the advantages of the new activation modes **E** and **F**. Except for good silicon affinity of the O atom, the catalytic species $[IPrH]^+[Carbamate]^-$ and IPr-CO_2 adduct are 6.0 and 5.5 kcal/mol, respectively, more thermodynamically stable than IPr (Scheme 3).[17] On the other hand, a structural change in the catalyst is very important for the high reactivity.[17] The structures in Figure 1 show clearly that the active site of IPr, i.e., the carbene carbon, is hiding inside and shielded by the large groups on the N atoms. Whereas for $[NHCH]^+[Carbamate]^-$ complex, the active site shifted to the O atom of the carbamate part, which is far away from the large arms of IPr. That is to say, the shielded active site of NHC is extended outside by forming $[NHCH]^+[Carbamate]^-$ complex. The O atom of the carbamate can do a nucleophilic attack nearly without steric effect. Test calculation shows that in **IPr-TS-Re-F**, the O atom of the carbamate will attack the Si center easily and form a penta-coordinated Si intermediate if the hydride acceptor CO_2 does not exist.[17] The N-heterocyclic olefin CO_2 adduct (NHO-CO_2), which has an extended active site, has much higher catalytic activity (10−200 times) than the corresponding NHC-CO_2 adduct does in the carboxylative cyclization of CO_2.[2i]

The barrier of **IPr-TS-Re-F** is lower than that of **IPr-TS-Re-E**. This may result from the larger negative atomic charges on the oxygen atom in **IPr-Carbamate** (−0.818) than that of **IPr-CO_2-Adduct** (−0.728). In **IPr-TS-Re-G** (28.2 kcal/mol), the N atom of Me_2NH activates the Si−H bond via S_N2 attack

DOI: 10.1021/jacs.5b03651
J. Am. Chem. Soc. 2015, 137, 10182−10189

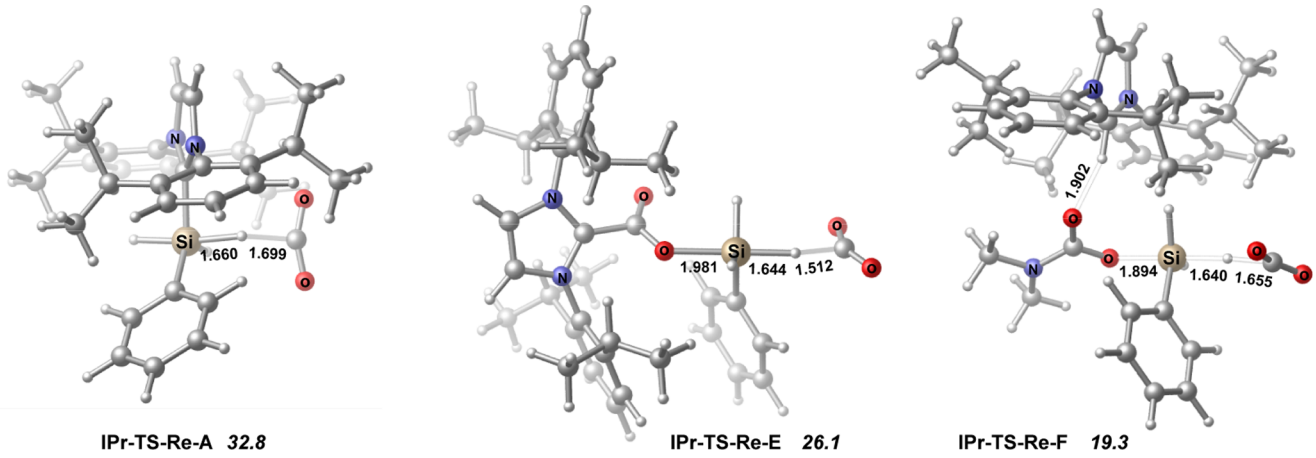

Figure 1. Optimized structures of representative activation modes (**IPr-TS-Re-A**, **IPr-TS-Re-E**, and **IPr-TS-Re-F**). The selected bond lengths are in Å. The relative free energies (ΔG_{sol}, 298 K, 1.0 atm) in THF are in kcal/mol.

Scheme 6. Calculated Reaction Pathways of IPr-Catalyzed Reductive Functionalization of CO_2 (Ar = 2,6-diisopropylphenyl)[a]

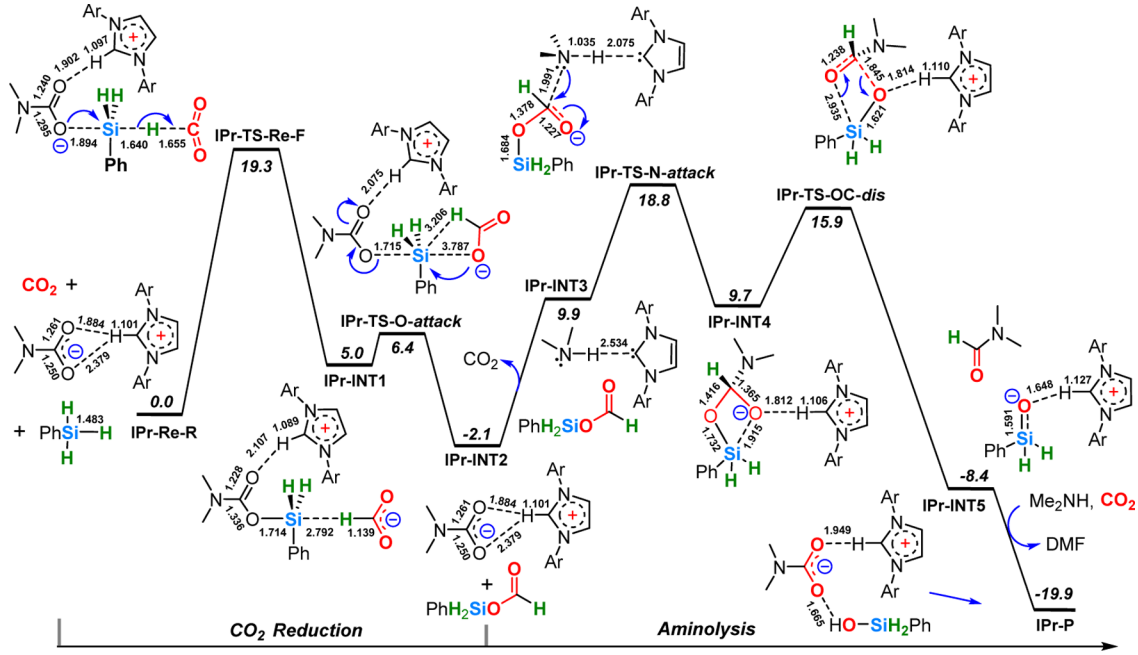

[a]The relative free energies (ΔG_{sol}, 298 K, 1.0 atm) in THF are in kcal/mol. The selected bond lengths are in Å. Calculated at the M06/(6-311++G** and 6-31G*) level.

under the promotion of IPr. Since the carbamate anion in $[IPrH]^+[Carbamate]^-$ is more reactive to activate Si−H bond, another version of activation mode **C**, **IPr-TS-Re-C′** (26.8 kcal/mol) is proposed. As expected, it is 8.7 kcal/mol lower than **IPr-TS-Re-C**. In addition, the barrier of IPr carbene insertion into the Si−H bond of $PhSiH_3$ is as high as 35.0 kcal/mol and can be safely excluded.[17]

Generally, the "partial model" is more favorable than the "whole model" due to the entropy effect. No matter which kind of model is used, the new activation mode **IPr-TS-Re-F** is the most favorable one.[17] In addition, this result is also supported by the calculations with several different methods.[17]

3.1.3. The Whole Reaction Pathways. Based on the best activation mode, the whole reaction pathways of reaction **1** were calculated (Scheme 6). The reduction starts from **IPr-Re-R**, which includes the $[IPrH]^+[Carbamate]^-$ salt complex, the free $PhSiH_3$, and CO_2 molecules. The reduction through **IPr-TS-Re-F** (19.3 kcal/mol) generates the intermediate **IPr-INT1** (5.0 kcal/mol). Next, the oxygen atom of the formate anion back bites the Si atom (**IPr-TS-O-*attack***, 6.4 kcal/mol), leading to the formoxysilane and $[IPrH]^+[Carbamate]^-$ salt **IPr-INT2** (−2.1 kcal/mol), and then, the aminolysis starts. Reversely along *Path-a* (Scheme 3), decarbonation of the $[IPrH]^+[Carbamate]^-$ salt in **IPr-INT2** leads to **IPr-INT3** (9.9 kcal/mol). Under the activation of IPr, Me_2NH attacks the carbonyl group of the formoxysilane (**IPr-TS-N-*attack*** 18.8 kcal/mol), leading to **IPr-INT4** (9.7 kcal/mol). The following O−C bond breaking via **IPr-TS-OC-*dis*** (15.9 kcal/mol) generates the formamide, and the siloxyl anion forms strong hydrogen bond with $IPrH^+$ cation (**IPr-INT5**, −8.4 kcal/mol). Subsequently, the free CO_2 and $HNMe_2$ combine with IPr to form $[IPrH]^+[Carbamate]^-$ salt complex and silanol (**IPr-P**, −19.8 kcal/mol), entering into the next catalytic cycle. The overall energy barrier is 20.9 kcal/mol, which is consistent with

DOI: 10.1021/jacs.5b03651
J. Am. Chem. Soc. 2015, 137, 10182−10189

the reaction conditions and the estimated energy barrier of 19.0 kcal/mol according to Eyring equation.[5b]

3.2. The Mechanism of Reaction 2. In the absence of amine, CO_2 will be reduced into methanol by silane with NHC catalyst.[3b] Based on the results shown in Scheme 3, if IMes is used, it will be trapped by forming IMes-CO_2 adduct. Therefore, the IMes-CO_2 adduct, the free Ph_2SiH_2, and CO_2 molecules (**IMes-Re-R**) were used as the zero energy reference. Experiments indicate that the first CO_2 reduction step is rate-determining.[5c] Therefore, the first reduction step was calculated in DMF, and five possible activation modes are shown in Scheme 7. Their barrier sequence is the same as that in reaction 1 (Scheme 4). **IMes-TS-Re-A** (29.7 kcal/mol), **IMes-TS-Re-A′** (29.0 kcal/mol), **IMes-TS-Re-B** (38.0 kcal/mol), and **IMes-TS-Re-C** (32.3 kcal/mol) are all disfavored.

Scheme 7. Calculated Transition States of Several Activation Modes for the First Reduction Step of Reaction 2 (Ar = 2,4,6-trimethylphenyl)[a]

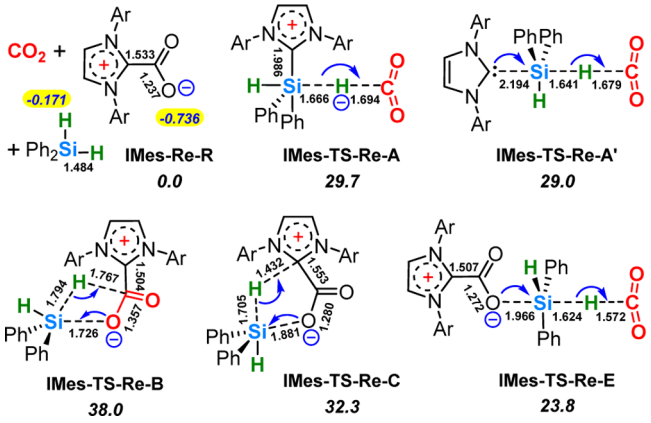

[a]Calculated at the M06/(6-311++G** and 6-31G*) level. The relative free energies (ΔG_{sol}, 298 K, 1.0 atm) in DMF are in kcal/mol.

In the best activation mode (**IMes-TS-Re-E**, 23.8 kcal/mol), the oxygen atom of the IMes-CO_2 adduct backside attacks the Si center and activates the Si−H bond. The more electrophilic free CO_2 molecule accepts the hydride without ring strain. By forming IMes-CO_2 adduct, the active site of IMes is extended outside. Consequently, the steric repulsions between the large arms of IMes and the silane in transition state can be avoided in some degree. The reduction barrier of 23.8 kcal/mol agrees well with the experimental conditions (RT, 6 h).[3b] These results indicate that IMes-CO_2 is the real catalytic species. In fact, the IMes-CO_2 adduct was used directly in reaction **2**.[3b] Other experimental[2b−e,k] and theoretical studies also show that NHC-CO_2 adducts may act as the real catalytic species in reactions.[25]

3.3. More Insights into the Catalytic Mechanisms. *3.3.1. From Uncatalyzed to Catalyzed: What Happened?* The pathway of the uncatalyzed reductive functionalization of CO_2 was explored as an ideal benchmark to discuss the NHC-catalyzed reaction.[17] In solvent, the amine-carbamic acid complex **Me_2NH-Carbamic-acid** is the global minimum (Scheme 8a), which has an equilibrium with the dimethylammonium dimethylcarbamate.[17] The best activation mode is **Me_2NH-TS-Re-F** (Scheme 8b), which is similar to **IPr-TS-Re-F**. When IPr is added into the system, more stable **IPr-Carbamate** will form. Consequently the global minimum of the system drops by 5.8 kcal/mol (Scheme 8a). However, the free energy of the reduction transition state **IPr-TS-Re-F** drops more by 12.4 kcal/mol (Scheme 8b). Thus, under the catalysis of IPr, the overall reaction barrier is decreased by 6.6 kcal/mol.

Scheme 8. (a) The Global Minimum Structures of the Uncatalyzed and Catalyzed Reactions and the Dissociation Energies of the Carbamate Anion, (b) The Transition States of the Uncatalyzed/Catalyzed Reactions and the Distortion Energies (DE), and (c) The Large Proton Affinity of IPr (Ar = 2,6-diisopropylphenyl)[a]

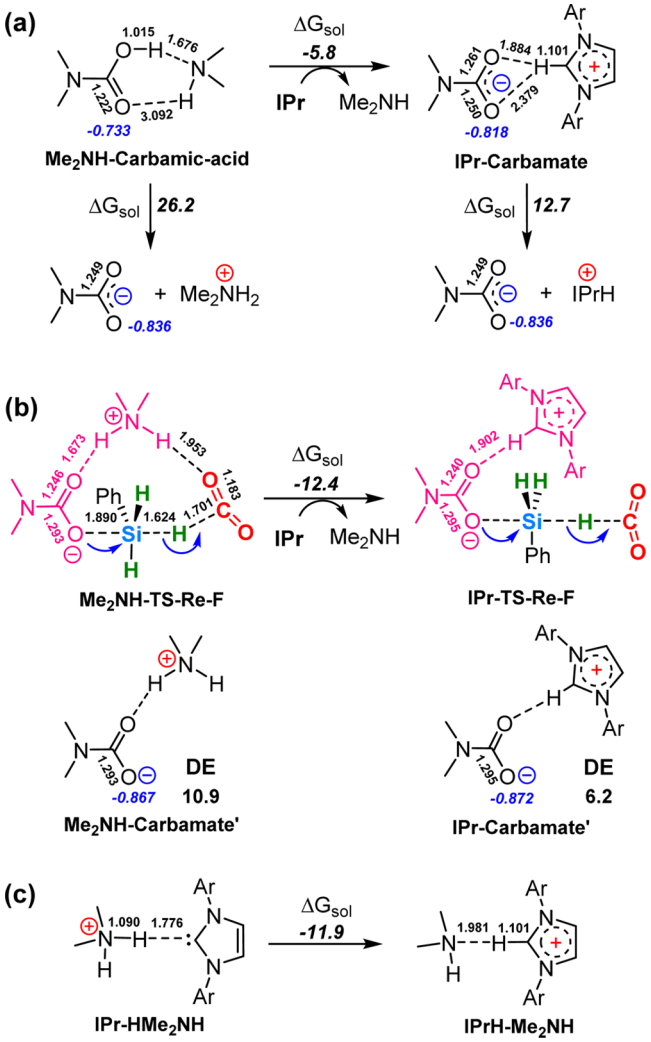

[a]Calculated at the M06/(6-311++G** and 6-31G*) level.

*3.3.2. Is the Carbamate Anion in **IPr-Carbamate** More Nucleophilic?* As shown in Scheme 8a, the dissociation free energy of **IPr-Carbamate** to $IPrH^+$ and the free carbamate anion is 12.7 kcal/mol, which is much lower than that of the **Me_2NH-Carbamic-acid** (26.2 kcal/mol). This result indicates that **IPr-Carbamate** is a relatively loose contact ion pair, in which the carbamate anion has higher reactivity to do nucleophilic attack. IPr has much higher proton affinity than Me_2NH does (Scheme 8c). Thus, in **IPr-Carbamate** the proton tightly binds to the carbene carbon atom and only has weaker interaction with the carbamate anion. Consequently, the carbamate anion has large negative charges on the O atom (−0.818 vs −0.733 in **$MeNH_2$-Carbamic-acid**). Therefore, the higher the proton affinity, the stronger the nucleophilicity of the carbamate anion.

DOI: 10.1021/jacs.5b03651
J. Am. Chem. Soc. 2015, 137, 10182−10189

3.3.3. How Does the Carbamate Anion in ***IPr-Carbamate*** *Lead to Higher Reactivity?* When the reactant complex is turning into the transition state, geometry distortions occur to reach the conformation required in the transition state, and the energy will rise. This distortion energy (DE)[26] is a key component of the reaction energy barrier. The DEs of **Me_2NH-Carbamic-acid** and **IPr-Carbamate** were estimated like this: for the two transition states shown in Scheme 8b, the silane and the CO_2 molecules were deleted with the rest part unchanged, giving **Me_2NH-Carbamate′** and **IPr-Carbamate′**. Then the single-point energies were calculated. Using the undistorted **Me_2NH-Carbamic-acid** and **IPr-Carbamate** as the zero-point references, respectively, the DEs were obtained. As shown in Scheme 8b, the DE of **IPr-Carbamate** is 4.7 kcal/mol lower than that of **Me_2NH-Carbamic-acid**. Thus, the carbamate anion in **IPr-Carbamate** is much easier to reach the conformation demanded in the transition state.

4. CONCLUSION

A comprehensive DFT study has been done on NHC-catalyzed reductive functionalization of CO_2. A new activation mode of the reduction step with a much lower energy barrier than those proposed previously was discovered. We found that in this reaction, NHC acts as neither a CO_2 nor a silane activator, but catalyzes the reaction by forming new species with higher catalytic activity, i.e., the ionic liquid $[NHCH]^+[Carbamate]^-$. In this loose contact ion pair, the negatively charged O atom of the carbamate anion becomes the new active site and is free to do a nucleophilic attack. This new activation mode follows the pattern of "S_N2@Si-Acceptor", in which the Si−H bond is activated via concerted backside S_N2 nucleophilic attack by the negatively charged O atom of the carbamate anion, and the leaving hydride is directly accepted by a free CO_2 molecule. The carbon atom of a free CO_2 is more electrophilic than those of the CO_2 moieties in NHC-CO_2 adduct and carbamate and can act as a more efficient hydride acceptor.

$[NHCH]^+[Carbamate]^-$ is superior to NHC in that (1) the ionic liquid $[NHCH]^+[Carbamate]^-$ is thermodynamically more stable than NHC; (2) the active site shifted from the deeply buried carbene carbon atom to the extended carbamate anion. Consequently, the steric effect between the large arms of NHC and the substrates in the transition state can be avoided in some degree; (3) the negatively charged O atom of the carbamate anion has good silicon affinity, which benefits the S_N2 attack to the Si atom. Ultimately, in this reaction, the high proton affinity of NHC is one of the main origins of the catalytic reactivity.

When amine is absent in the reaction, the NHC-CO_2 adduct is revealed to be the real catalytic species, in which the negatively charged O atom becomes the new active site, and the best activation mode in the reaction also follows the pattern of "S_N2@Si-Acceptor".

Our results present deeper insights into the real role of the NHC catalyst in these reactions and will challenge the generally accepted mechanisms. This new mechanistic understanding is important both for improvement of CO_2 transformation reactions and for NHC catalyst design in the future and also provides new clue on the mechanistic study of guanidine-catalyzed reactions.[27]

■ ASSOCIATED CONTENT

Supporting Information

The Supporting Information is available free of charge on the ACS Publications website at DOI: 10.1021/jacs.5b03651.

The calculation details, test calculations, selected IRC calculations and the calculated total energies and geometrical coordinates (PDF)

■ AUTHOR INFORMATION

Corresponding Author

*liyuxue@sioc.ac.cn

Notes

The authors declare no competing financial interest.

■ ACKNOWLEDGMENTS

This project is supported by the National Basic Research Program of China (973 Program, no. 2015CB856600) and the Natural Science Foundation of China (grant nos. 21372249, 21172248, 21402229, and 21421091).

■ REFERENCES

(1) (a) International Energy Agency. *Tracking Industrial Energy Efficiency and CO_2 Emissions*; OECD/IEA; Paris, France, 2007. (b) Sakakura, T.; Choi, J. C.; Yasuda, H. *Chem. Rev.* **2007**, *107*, 2365. (c) Darensbourg, D. J. *Chem. Rev.* **2007**, *107*, 2388. (d) Sakakura, T.; Kohno, K. *Chem. Commun.* **2009**, 1312. (e) Aresta, M. *Carbon Dioxide as Chemical Feedstock*; Wiley-VCH Verlag GmbH: Weinheim, 2010. (f) Huang, K.; Sun, C.-L.; Shi, Z.-J. *Chem. Soc. Rev.* **2011**, *40*, 2435. (g) Lu, X. B.; Ren, W. M.; Wu, G. P. *Acc. Chem. Res.* **2012**, *45*, 1721. (h) Tlili, A.; Blondiaux, E.; Frogneux, X.; Cantat, T. *Green Chem.* **2015**, *17*, 157.

(2) Selected works on NHC-catalyzed CO_2 transformation: (a) Marion, N.; Díez-González, S.; Nolan, S. P. *Angew. Chem., Int. Ed.* **2007**, *46*, 2988. (b) Zhou, H.; Zhang, W.-Z.; Liu, C.-H.; Qu, J.-P.; Lu, X.-B. *J. Org. Chem.* **2008**, *73*, 8039. (c) Kayaki, Y.; Yamamoto, M.; Ikariya, T. *Angew. Chem., Int. Ed.* **2009**, *48*, 4194. (d) Gu, L.; Zhang, Y. *J. Am. Chem. Soc.* **2009**, *132*, 914. (e) Zhang, Y.; Chan, J. Y. G. *Energy Environ. Sci.* **2010**, *3*, 408. (f) Nair, V.; Varghese, V.; Paul, R. R.; Jose, A.; Sinu, C. R.; Menon, R. S. *Org. Lett.* **2010**, *12*, 2653. (g) Ajitha, M. J.; Suresh, C. H. *J. Org. Chem.* **2011**, *77*, 1087. (h) Chiang, P.-C.; Bode, J. W. *Org. Lett.* **2011**, *13*, 2422. (i) Wang, Y. B.; Wang, Y. M.; Zhang, W. Z.; Lu, X. B. *J. Am. Chem. Soc.* **2013**, *135*, 11996. (j) Hopkinson, M. N.; Richter, C.; Schedler, M.; Glorius, F. *Nature* **2014**, *510*, 485. (k) Yang, L.; Wang, H. *ChemSusChem* **2014**, *7*, 962. (l) Fontaine, F.-G.; Courtemanche, M.-A.; Légaré, M.-A. *Chem. - Eur. J.* **2014**, *20*, 2990. (m) Fernández-Alvarez, F. J.; Aitanib, A. M.; Oro, L. A. *Catal. Sci. Technol.* **2014**, *4*, 611.

(3) Main experimental works related to our DFT study: (a) Jacquet, O.; Gomes, C. D. N.; Ephritikhine, M.; Cantat, T. *J. Am. Chem. Soc.* **2012**, *134*, 2934. (b) Riduan, S. N.; Zhang, Y.; Ying, J. Y. *Angew. Chem., Int. Ed.* **2009**, *48*, 3322.

(4) (a) Jacquet, O.; Das Neves Gomes, C.; Ephritikhine, M.; Cantat, T. *ChemCatChem* **2013**, *5*, 117. (b) Jacquet, O.; Frogneux, X.; Das Neves Gomes, C.; Cantat, T. *Chem. Sci.* **2013**, *4*, 2127. (c) Blondiaux, E.; Pouessel, J.; Cantat, T. *Angew. Chem., Int. Ed.* **2014**, *53*, 12186. (d) Das, S.; Bobbink, F. D.; Laurenczy, G.; Dyson, P. J. *Angew. Chem., Int. Ed.* **2014**, *53*, 12876. (e) Lu, Z.; Hausmann, H.; Becker, S.; Wegner, H. A. *J. Am. Chem. Soc.* **2015**, *137*, 5332.

(5) DFT calculation works on NHC-catalyzed CO_2 transformation: (a) Huang, F.; Lu, G.; Zhao, L.; Li, H.; Wang, Z.-X. *J. Am. Chem. Soc.* **2010**, *132*, 12388. (b) Wang, B.; Cao, Z. *RSC Adv.* **2013**, *3*, 14007. (c) Riduan, S. N.; Ying, J. Y.; Zhang, Y. *ChemCatChem* **2013**, *5*, 1490.

(6) Selected works of guanidine organocatalysis: (a) Barbarini, A.; Maggi, R.; Mazzacani, A.; Mori, G.; Sartori, G.; Sartorio, R. *Tetrahedron Lett.* **2003**, *44*, 2931. (b) Gao, J. A.; He, L. N.; Miao, C. X.; Chanfreau, S. *Tetrahedron* **2010**, *66*, 4063. (c) Villiers, C.;

DOI: 10.1021/jacs.5b03651
J. Am. Chem. Soc. 2015, 137, 10182−10189

Dognon, J.-P.; Pollet, R.; Thuéry, P.; Ephritikhine, M. *Angew. Chem., Int. Ed.* **2010**, *49*, 3465. (d) Della Ca, N.; Gabriele, B.; Ruffolo, G.; Veltri, L.; Zanetta, T.; Costa, M. *Adv. Synth. Catal.* **2011**, *353*, 133. (e) Yang, Z. Z.; He, L. N.; Zhao, Y. N.; Li, B.; Yu, B. *Energy Environ. Sci.* **2011**, *4*, 3971. (f) Fu, X.; Tan, C.-H. *Chem. Commun.* **2011**, *47*, 8210. (g) Gomes, C. D. N.; Jacquet, O.; Villiers, C.; Thuéry, P.; Ephritikhine, M.; Cantat, T. *Angew. Chem., Int. Ed.* **2012**, *51*, 187.

(7) (a) Hohenberg, P.; Kohn, W. *Phys. Rev.* **1964**, *136*, B864−B871. (b) Kohn, W.; Sham, L. *Phys. Rev.* **1965**, *140*, A1133−A1138.

(8) (a) Zhao, Y.; Truhlar, D. G. *J. Phys. Chem. A* **2006**, *110*, 13126. (b) Zhao, Y.; Truhlar, D. G. *J. Chem. Phys.* **2006**, *125*, 194101. (c) Zhao, Y.; Truhlar, D. G. *Theor. Chem. Acc.* **2008**, *120*, 215.

(9) Frisch, M. J.; Trucks, G. W.; Schlegel, H. B.; Scuseria, G. E.; Robb, M. A.; Cheeseman, J. R.; Scalmani, G.; Barone, V.; Mennucci, B.; Petersson, G. A.; Nakatsuji, H.; Caricato, M.; Li, X.; Hratchian, H. P.; Izmaylov, A. F.; Bloino, J.; Zheng, G.; Sonnenberg, J. L.; Hada, M.; Ehara, M.; Toyota, K.; Fukuda, R.; Hasegawa, J.; Ishida, M.; Nakajima, T.; Honda, Y.; Kitao, O.; Nakai, H.; Vreven, T.; Montgomery, J. A., Jr.; Peralta, J. E.; Ogliaro, F.; Bearpark, M.; Heyd, J. J.; Brothers, E.; Kudin, K. N.; Staroverov, V. N.; Kobayashi, R.; Normand, J.; Raghavachari, K.; Rendell, A.; Burant, J. C.; Iyengar, S. S.; Tomasi, J.; Cossi, M.; Rega, N.; Millam, N. J.; Klene, M.; Knox, J. E.; Cross, J. B.; Bakken, V.; Adamo, C.; Jaramillo, J.; Gomperts, R.; Stratmann, R. E.; Yazyev, O.; Austin, A. J.; Cammi, R.; Pomelli, C.; Ochterski, J. W.; Martin, R. L.; Morokuma, K.; Zakrzewski, V. G.; Voth, G. A.; Salvador, P.; Dannenberg, J. J.; Dapprich, S.; Daniels, A. D.; Farkas, Ö.; Foresman, J. B.; Ortiz, J. V.; Cioslowski, J.; Fox, D. J. *Gaussian 09*, revision A.02; Gaussian, Inc.: Wallingford, CT. 2009.

(10) Marenich, A. V.; Cramer, C. J.; Truhlar, D. G. *J. Phys. Chem. B* **2009**, *113*, 6378.

(11) (a) Fukui, K. *J. Phys. Chem.* **1970**, *74*, 4161. (b) Fukui, K. *Acc. Chem. Res.* **1981**, *14*, 363.

(12) Legault, C. *CYLview, 1.0b*; Université de Sherbrooke: Quebec, Canada, 2009.

(13) (a) Benson, S. W. *The Foundations of Chemical Kinetics*; R. E. Krieger: Malabar, FL, 1982. (b) Liu, Q.; Lan, Y.; Liu, J.; Li, G.; Wu, Y.-D.; Lei, A. *J. Am. Chem. Soc.* **2009**, *131*, 10201. (c) Schoenebeck, F.; Houk, K. N. *J. Am. Chem. Soc.* **2010**, *132*, 2496. (d) Liu, B.; Gao, M.; Dang, L.; Zhao, H.; Marder, T. B.; Lin, Z. *Organometallics* **2012**, *31*, 3410.

(14) Selected works about carbamate formation: (a) Knausz, D.; Meszticzky, A.; Szakács, L.; Csákvári, B.; Ujszászy, K. *J. Organomet. Chem.* **1983**, *256*, 11. (b) Schroth, W.; Andersch, J. *Synthesis* **1989**, *1989*, 202. (c) Schroth, W.; Schadler, H. D.; Andersch, J.; Wiegeleben, A.; Wedler, W.; Krahnstover, J.; Radeglia, R.; Kolbe, A.; Schwarz, W. *Z. Chem.* **1989**, *29*, 129. (d) Littel, R. J.; Versteeg, G. F.; van Swaaij, W. P. M. *Chem. Eng. Sci.* **1992**, *47*, 2037. (e) Dell'Amico, D. B.; Calderazzo, F.; Labella, L.; Marchetti, F.; Pampaloni, G. *Chem. Rev.* **2003**, *103*, 3857. (f) Kreher, U. P.; Rosamilia, A. E.; Raston, C. L.; Scott, J. L.; Strauss, C. R. *Molecules* **2004**, *9*, 387. (g) Maloschik, E.; Moertl, M.; Szekacs, A. *Anal. Bioanal. Chem.* **2010**, *397*, 537. (h) Mase, N.; Horibe, T. *Org. Lett.* **2013**, *15*, 1854.

(15) (a) Kreher, U.; Raston, C. L.; Strauss, C. R.; Nichols, P. J. *Acta Crystallogr., Sect. E: Struct. Rep. Online* **2002**, *58*, o948. (b) Aresta, M.; Ballivet-Tkatchenko, D.; Dell'Amico, D. B.; Bonnet, M. C.; Boschi, D.; Calderazzo, F.; Faure, R.; Labella, L.; Marchetti, F. *Chem. Commun.* **2000**, 1099. (c) Jiang, H.; Zhang, S.; Xu, Y. *Afr. J. Pure Appl. Chem.* **2009**, *3*, 126. (d) Tiritiris, I.; Kantlehner, W. *Z. Naturforsch., B: J. Chem. Sci.* **2011**, *66*, 164.

(16) (a) Jamróz, M.; Dobrowolski, J. C.; Borowiak, M. A. *J. Mol. Struct.* **1997**, *404*, 105. (b) da Silva, E. F.; Svendsen, H. F. *Ind. Eng. Chem. Res.* **2006**, *45*, 2497. (c) Yu, G. R.; Zhang, S. J.; Yao, X. Q.; Zhang, J. M.; Dong, K.; Dai, W. B.; Mori, R. *Ind. Eng. Chem. Res.* **2006**, *45*, 2875. (d) Mindrup, E. M.; Schneider, W. F. *ChemSusChem* **2010**, *3*, 931. (e) Eger, W. A.; Genest, A.; Rieger, B.; Rosch, N. *ChemSusChem* **2012**, *5*, 1967.

(17) For details see Supporting Information.

(18) (a) Holloczki, O.; Gerhard, D.; Massone, K.; Szarvas, L.; Nemeth, B.; Veszpremi, T.; Nyulaszi, L. *New J. Chem.* **2010**, *34*, 3004. (b) Hunt, P. A.; Kirchner, B.; Welton, T. *Chem. - Eur. J.* **2006**, *12*, 6762. (c) Hunt, P. A.; Gould; Ian, R.; Kirchner, B. *Aust. J. Chem.* **2007**, *60*, 9. (d) Hollóczki, O.; Malberg, F.; Welton, T.; Kirchner, B. *Phys. Chem. Chem. Phys.* **2014**, *16*, 16880. (e) Dai, Y. F.; Qu, Y. X.; Wang, S.; Wang, J. D. *Comput. Theor. Chem.* **2015**, *1055*, 33. (f) Pi, C. F.; Yu, X. L.; Zheng, W. J. *Eur. J. Inorg. Chem.* **2015**, *10*, 1804. (g) Hunt, P. A.; Ashworth, C. R.; Matthews, R. P. *Chem. Soc. Rev.* **2015**, *44*, 1257.

(19) Selected works on NHC-CO_2 adducts: (a) Kuhn, N.; Steimann, M.; Weyers, G. *Z. Naturforsch., B: J. Chem. Sci.* **1999**, *54*, 427. (b) Holbrey, J. D.; Reichert, W. M.; Tkatchenko, I.; Bouajila, E.; Walter, O.; Tommasi, I.; Rogers, R. D. *Chem. Commun.* **2003**, 28. (c) Duong, H. A.; Tekavec, T. N.; Arif, A. M.; Louie, J. *Chem. Commun.* **2004**, 112. (d) Van Ausdall, B. R.; Poth, N. F.; Kincaid, V. A.; Arif, A. M.; Louie, J. *J. Org. Chem.* **2011**, *76*, 8413. (e) Cabaço, M. I.; Besnard, M.; Danten, Y.; Coutinho, J. A. P. *J. Phys. Chem. A* **2012**, *116*, 1605.

(20) Selected works on Si-H activation via S_N2 mechanisms: (a) Bento, A. P.; Bickelhaupt, F. M. *J. Org. Chem.* **2007**, *72*, 2201. (b) Rendler, S.; Oestreich, M. *Angew. Chem., Int. Ed.* **2008**, *47*, 5997. (c) Pérez, M.; Caputo, C. B.; Dobrovetsky, R.; Stephan, D. W. *Proc. Natl. Acad. Sci. U. S. A.* **2014**, *111*, 10917. (d) Wen, M. W.; Huang, F.; Lu, G.; Wang, Z.-X. *Inorg. Chem.* **2013**, *52*, 12098.

(21) (a) Hiyama, T.; Hatanaka, Y. *Pure Appl. Chem.* **1994**, *66*, 1471. (b) Lipshutz, B. H.; Shin, Y. J. *Tetrahedron Lett.* **2001**, *42*, 5629.

(22) Reed, A. E.; Weinstock, R. B.; Weinhold, F. *J. Chem. Phys.* **1985**, *83*, 735.

(23) Luo, Y. R. *Comprehensive Handbook of Chemical Bond Energies*; CRC Press, Boca Raton, FL, 2007, Chapter 9, p 455. The O−Si bond energy is from the Me_3Si−OMe bond (p 462), the N−Si bond energy is from the Me_3Si−NMe_2 bond (p 463), the C−Si bond energy is from the Me_3Si−CH_3 bond (p 461), and the F−Si bond energy is from the Me_3Si−F bond (p 464).

(24) (a) Brook, A. G. *Acc. Chem. Res.* **1974**, *7*, 77. (b) Peterson, D. J. *J. Org. Chem.* **1968**, *33*, 780.

(25) (a) Singh, A.; Goel, N. *Struct. Chem.* **2014**, *25*, 1245. (b) Li, W.; Huang, D.; Lv, Y. *RSC Adv.* **2014**, *4*, 17236.

(26) (a) Legault, C. Y.; Garcia, Y.; Merlic, C. A.; Houk, K. N. *J. Am. Chem. Soc.* **2007**, *129*, 12664. (b) Hayden, A. E.; Houk, K. N. *J. Am. Chem. Soc.* **2009**, *131*, 4084.

(27) Unpublished results.

DOI: 10.1021/jacs.5b03651
J. Am. Chem. Soc. 2015, 137, 10182−10189